Catalysis Science & Technology

Accepted Manuscript

ROYAL SOCIETY OF CHEMISTRY

www.rsc.org/catalysis

Catal. Sci. Technol.

RSCPublishing

ARTICLE

Role of the support on the performance and stability of Pt-based catalysts for furfural-acetone adducts hydrodeoxygenation

Cite this: DOI: 10.1039/xoxxoooooox

Received ooth January 2014,
Accepted ooth January 2014

DOI: 10.1039/xoxxoooooox

www.rsc.org/

L. Faba[a], E. Díaz[a], S. Ordóñez[a]

The role of the support on the catalytic activity, product distribution, and stability of supported Pt catalysts in the hydrodeoxygenation of acetone-furfural condensation adduct is studied in the present work. Supports as ZSM-5, L and Y zeolites, high surface area graphites and activated carbons have been tested, modelling the results with a previously proposed reaction network. The analysis of the kinetic constants shows that first steps (hydrogenation of aliphatic multiple bonds) are structure sensitive, mostly depending on metal dispersion, whereas those steps involving ring opening and HDO of the resulting diols present a more complex chemistry, involving the morphological and acid-base properties of the support. Concerning the catalyst stability, the formation of carbonaceous deposits is the main deactivation cause.

Introduction

Production of renewable liquid fuels from biomass resources is nowadays of key interest. Among the different possibilities, and considering the high-energy demanding of pyrolysis or gasification technologies, liquid phase processes constitute a very promising alternative.[1] First approach to these technologies was reported by *Dumesic and co-workers*, proposing a four-step catalytic process for obtaining high-quality diesel fuel from hemicellulosic material.[2] The hydrolysis and subsequent dehydration of hemicellulose yielding furfural and hydroximethylfurfural is the first step of this process, being performed both with homogeneous or heterogeneous catalysts.[3,4] The combustion enthalpy and physical properties of these cyclic-aldehydes are enhanced by increasing the length of the carbon chain in a second step. The aldol condensation with acetone is the one of the most common reactions to obtain adducts with 8-13 carbon atoms.[2,5-8]

Condensation adducts are over-functionalized molecules and their conversion into valuable liquid fuels requires a final step of hydrogenation and oxygen removal (hydrodeoxygenation, HDO) to obtain the corresponding n-alkanes. First references of HDO process were applied to oil-derivatives using different metals supported on Al_2O_3 at high pressures (623 K and 13.6 MPa).[9] The high complexity of this process (involving different steps of hydrogenation, dehydration, cycle breaking-up, etc.) justifies that the HDO of biomass-derived condensation adducts (2-methylpentanal or furfural) was usually divided into two processes: a first one in aqueous phase at mild conditions and a more severe second step using organic solvents.[10-12]

We have studied in a previous work the HDO of furfural-acetone condensation adducts into n-alkanes as a one-step process in organic phase.[13] The complex mechanism of this reaction was thoroughly analysed, studying the influence of different reaction parameters, such as the temperature and the active metal. The proposed kinetic model involves a network of series/parallel first-order reactions, following the reaction network showed in Scheme 1. Platinum was identified as the most active metal, obtaining selectivities of n-octane higher than 35 % when reactions are carried out at 493 K for 24 h.[13]

The activity of this metal is strongly affected by several parameters such as the metal precursor and the impregnation method used to incorporate the noble metals onto the support, as well as the properties of these supports. Several studies demonstrate that ion exchange and incipient wetness result in a very uniform distribution of metal nanoparticles on a wide variety of both organic and inorganic supports.[14] Concerning the metal precursors, chlorides and nitrates are the most commonly used salts in catalyst preparations because they are relatively inexpensive and highly water soluble. However, there is not good agreement about the most effective one and opposite effects in hydrogenation studies have been reported. Residual chloride can limit the metal dispersion and catalyse some side-reactions but can also favour metal interactions that modify the pretreatment temperature and enhance the catalytic performance.[15,16]

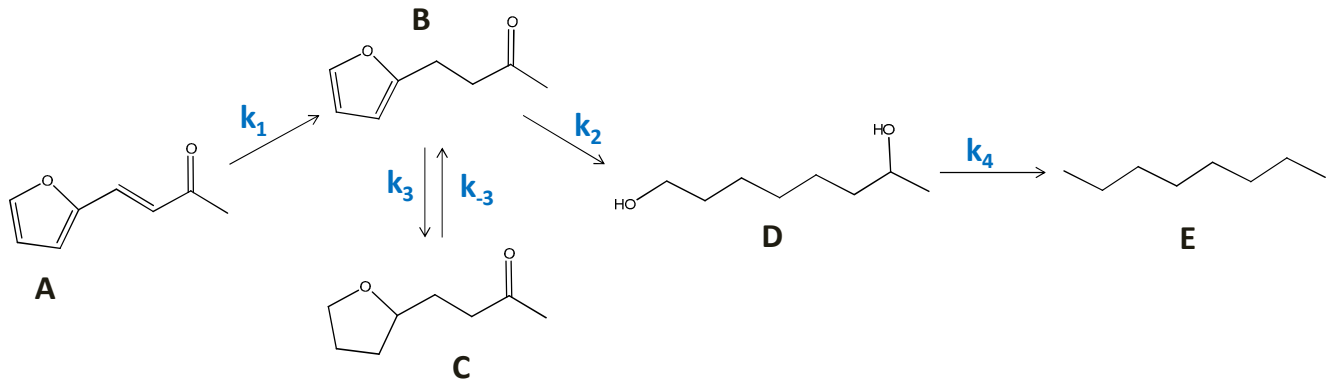

Scheme 1: Reaction mechanism proposed to the hydrodeoxygenation of the furfuryldenacetone. Symbols: "A" furfuryldeneacetone; "B", 4-furfuryl-2-butanone; "C", 4-tetrahydrofurfuryl-2-butanone; "D", 1,7-octanodiol, "E", n-octane.

Concerning the supports, their morphological and physic-chemical properties (acid sites, adsorption capacity) influence, to a different extent, the different reaction steps (hydrogenation, ring opening, dehydration), and can create active sites for catalysing side reactions that decrease selectivities and lead to catalytic deactivation.[17] Zeolites can be considered as good supports because of their structure ordering at the nanometre scale and they were successfully used in the hydrogenation of similar compounds, as citral or levulinic acid.[18,19] However, their small pores can also lead to diffusional limitations in reactions with larger molecules. Concerning the organic supports, several types of carbons have been applied in different hydrogenation reactions.[20] Active carbons and graphites are the most used carbons but the activity of these materials is strongly conditioned by the surface oxygen groups that can have a positive or negative effect as anchoring sites.[21]

The main scope of this work is to provide new insights the role of different catalyst properties (such as metal dispersion, morphology or surface acidity) on the catalyst performance (activity, selectivity and reusability) of Pt-based catalysts. To the best of our knowledge, there is a lack of mechanistic studies on this reaction, being even more scarce those studies looking at deactivation causes.

Experimental methodology

Catalysts preparation

A 0.5 % Pt/Al_2O_3 commercial catalyst supplied by BASF was used a reference catalyst. Concerning the inorganic materials, zeolites (NaY, KL, Na-ZSM-5 (Si/Al=25) and Na-ZSM5 (Si/Al=11)) were supplied by Zeolist, whereas MgZr was prepared in the laboratory from the corresponding nitrate precursors by the co-precipitation method deeply explained in a previous work.[5] High surface area graphites (HSAG-500) and active carbons (AC, GF 40) were supplied by Timcal S.A. and Norit, respectively. Pt-catalysts were prepared by using two different preparation procedures (ion exchange and incipient wetness) combined with two different metal precursors, both supplied by Aldrich: $Pt(NH_3)_4(NO_3)_2$ and $Pt(NH_3)_4Cl_2$.

Catalysts obtained by ion exchange were prepared by suspending 5 g of the support in 250 mL of an aqueous solution of metal precursor. The solutions were prepared considering a final metal loading of 1% by solving 0.09 g or 0.1 g of chloride or nitrate salt, respectively. The ion exchange was carried out in a rotavapor at 343 K for 24 h and under vacuum conditions, in order to remove completely the solvent. Incipient wetness method was used considering the specific pore volume of each support.

Solids prepared by both methods were washed and filtered in order to remove possible rests of nitrates or chlorines. Catalysts were dried at 373 K and heated in He flow at a temperature rate of 5 K/min until 873 K, holding this temperature during 2 h. All the materials were activated before any characterization or activity test at 473 K for 2 h under flowing hydrogen gas.

Catalysts characterization

Morphological properties were determined by using nitrogen physisorption at 77 K in a Micromeritics ASAP 2020 analyser using the BET method for the specific surface area and the BJH approach to determine the pore volume and diameter. Platinum dispersion as well as platinum crystallite sizes were determining by transmission electron microscopy (TEM) in a MET JEOL-2000 EX-II microscope. Other techniques to measure the metal dispersion are not applied in order to be congruent with all the supports studied in this work. XRD technique cannot be used to measure the Pt dispersion on alumina and some zeolites because the main peak of Pt (2θ = 39.7°) match up with the (222) plane of Al_2O_3 and LTL zeolite. On the other hand, chemisorption is not used to make easier the comparison among fresh and spent catalysts results, taking into account that coke deposits prevent the CO adsorption. The metal loading of the catalysts was determined by ICP-OES using a HP 7500c spectrometer.

The strength and distribution of the acid sites were determined by temperature programmed desorption of preadsorbed NH_3 in a Micromeritics TPD/TPR 2900. Samples (10 mg) were pre-treated in He at 823 K for 2.5 h and exposed to a NH_3 stream (2.5% NH_3 in He) at 323 K until saturation coverage was reached. Weakly adsorbed NH_3 was removed by flushing with He at the same temperature for about 1.30 h. The temperature was then increased at a linear rate of 5 K/min from 293 K to 723 K and the signal of NH_3 desorbed was monitored by mass spectrometry.

Reaction studies

Reactions were carried out in a 0.5 L stirred batch autoclave reactor (Autoclave Engineers EZE Seal) equipped with a PID temperature controller and a back pressure regulator. The reactor was loaded with 0.25 L of a hexane solution of 0.42 g of furfuryldeneacetone (Alfa Aesar, 98 %). The catalyst (60 mg) was added (with an average particle diameter of 50-80 μm) and air was purged out by adding nitrogen up to 1.5 MPa for three times before starting reaction. The C8 loading and the reactant/catalyst ratio were chosen considering the previous results obtained in the aldolization studies.[5] The reactor was pressurized to 2.5 MPa of H_2, stirred at 1000 rpm and heated to 493 K, reaching a final pressure of 5.5 MPa.

Samples were withdrawn from the sampling port, filtered and analysed by capillary GC-FID in a Shimadzu GC-2010, using a CP-Sil 5 capillary column as a stationary phase. Peak assignment was performed by GC-MS and responses were determined using appropriate standards. The structure of the different intermediates is shown in Scheme 1. Due to the complexity of the chemical nomenclature of each compound, they were labeled with a capital letter: furfuryldeneacetone (A); 4-furfuryl-2-butanone (B); 4-tetrahydro-furfuryl-2-butanone (C); 1,7-octanodiol (D); n-octane (E). Activity results were analyzed in terms of the evolution of the yield for each compound, being this parameter calculated as the ratio between the concentrations of each compound divided by the decrease in the reactant concentration.

Deactivation studies were carried out by recovering the spent catalysts after the first 24 hours of reaction. The catalyst was filtered, washed, dried at 373 K and used in five subsequent batches with fresh reactants, and keeping out the same conditions of temperature, concentrations, pressure, stirring and organic/catalyst ratio.

Results and discussion

Optimization of preparation method

First studies were carried out in order to optimize the catalyst preparation method and the metal precursor. ZSM-5 zeolite (with a SiO_2/Al_2O_3 ratio of 25) was chosen as support. Catalyst prepared by ion exchange method was labelled with "1", whereas those prepared by incipient wetness were labelled as "2". Letters "A" or "B" was added in order to identify the chlorine or nitrate precursor, respectively. As prepared catalysts were analysed by different characterization techniques and main results are summarized in Table 1. As it could be expected, morphological parameters are highly similar for the four Pt/ZSM-5 catalysts studied, with surface areas higher than 300 m^2/g, and values of pore volumes and diameters much smaller than those obtained with the alumina support. There are not important differences in terms of metal loading, with the highest values obtained when nitrate precursor is used. Metal dispersion is lower than 25 % in the four cases. These values are in good agreement with values reported in the literature for Pt supported catalysts prepared by similar methods.[22,23] Ion exchange allows obtaining catalysts with higher metal dispersion, mainly when nitrate precursor was used. This behaviour was previously observed in studies about the influence of different impregnation methods on the properties of zeolites.[24] Main micrographs obtained by TEM analyses are shown in the Supplementary Information (Fig. S1-S2), observing in all the cases well defined cubic metal particles. This morphology was previously observed when metals are confined between the zeolitic planes.[25,26] Histograms of metal particle diameter are superimposed on micrographs. It should be noted that although most of the crystallites present larger sizes than support pore diameter, there are also smaller particles, which can be located inside the porous structure.

Main differences were obtained in the concentration and distribution of the acidity: the lowest amount of acid sites was obtained with the Pt/ZSM-5 (1.A), leading to a wide distribution of acid strengths. On the other hand, materials prepared by incipient wetness do not show so strong sites but the global concentration of acid sites is largely higher. The high concentration of acid sites at increasing metal loading for the Pt catalysts supported on zeolites was previously reported.[27]

In general terms, reaction profiles obtained with the four

Table 1: Morphological and physico-chemical parameters. *Data of Pt/Al_2O_3 adapted from *ref. 13*.

	N_2 physisorption			Metal loading, ICP-MS (%)	Metal dispersion, TEM (%)	Acidity, NH_3-TPD (μmol/g, K)		
	S_{BET} (m^2/g)	d_p (nm)	v_p (cm^3/g)			Weak (< 450 K)	Medium (450 - 650 K)	Strong (> 650 K)
Pt/Al_2O_3*	116	17.0	0.49	0.5	23.9	798	119	-
Pt/ZSM-5 (1.A)	324	5.2	0.07	0.85	10.2	712	201	215
Pt/ZSM-5 (1.B)	327	5.7	0.09	0.91	9.5	2572	625	1332
Pt/ZSM-5 (2.A)	335	5.4	0.07	0.87	7.1	3804	582	-
Pt/ZSM-5 (2.B)	305	5.2	0.07	0.93	5.4	1494	430	-
Pt/ZSM-5 (Si/Al 11)	287	4.9	0.05	0.85	12.8	1280	1320	-
Pt/L	302	17.8	0.08	0.80	11.0	1177	-	-
Pt/Y	220	24.3	0.06	0.82	12.1	901	-	-
Pt/MgZr	34	27.2	0.26	0.74	10.4	225	206	-
Pt/HSAG500	498	7.6	0.67	0.86	8.6	30	36	7
Pt/AC (IE)	1214	2.8	0.17	0.71	14.3	129	146	-
Pt/AC (WI)	1716	1.9	0.59	0.53	21.3	18	71	-
Pt/MgZr/HSAG500	234	10.1	0.50	0.58	-	243	230	-

catalysts are qualitatively similar, following the trends depicted in Figure 1. These profiles show a fast disappearance of the reactant, reaching in all the cases C8 conversions higher than 95 % in less than 3 hours. This decrease is related to the appearance of the first intermediate ("B"). This compound reaches a maximum, after which its concentration slightly decreases because of the appearance of the other intermediates. More than 6 hours of reaction are needed before detecting the n-alkane and after 24 hours the maximum n-alkane yield is 6.3 %.

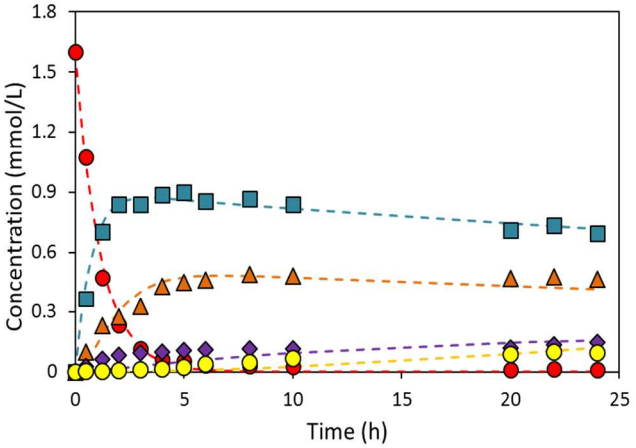

Figure 1: Concentration profiles obtained in HDO of C8-conden-sated adduct catalysed by Pt/ZSM-5(1.A) at 393 K and 5.5 MPa of H_2. Symbols: (●) "A"; (■) "B"; (▲) "C"; (◆) "D"; (●) "E"

In order to compare the results obtained with the different catalysts, yields at 50 % of C8 conversion and after 24 hours of hydrodeoxygenation at 493 K with these four ZSM5-based catalysts are shown in Figure 2, whereas yields at 95 % of conversion are provided in the Fig. S3**.** The performance of the commercial Pt/Al_2O_3 is also plotted for comparison purposes. At 50 % of conversion, final carbon balances were, in all cases, higher than 85 %. Pt/ZSM-5 1.A shows the highest activity, even more than the Pt/Al_2O_3, and the highest yields of "C" and "D" intermediates, whereas other materials show much higher yield of the first intermediate. Concerning the n-octane, it was almost negligible in all the cases, since longer reaction times are needed to produce the alkane in significant amounts.

After 24 hours, conversions higher than 95 % were obtained in all the cases, being the "C" intermediate the major product. In a previous work,[13] it was demonstrated that the intermediate "C" is a lateral product, not undergoing further hydrogenation. The high yield to the "C" intermediate, mainly with the Pt/ZSM-5 (2.A), contrasts with the value previously obtained with Pt/Al_2O_3. The high concentration of this intermediate can be related to the higher acidity of these materials. There is not good agreement about the role of acidity in this type of reactions. On the one hand, acidity is identified as the key parameter in hydrogenations of different aromatic compounds, regardless of the considered metal.[28] On the other hand, it is also observed that the acidity stabilizes cyclic structures,[29] preventing the formation of linear alkanes. Looking at the final yield of alkane, best results were obtained with the Pt/ZSM-5-1.A (6.3 %), catalyst which combines the highest metal dispersion and the lowest concentration of acid sites, as summarised in Table 1. This yield is, in any case, considerably lower than the final yield obtained with the alumina (27.8 %), suggesting a negative effect of the acidity of the support.

Performance of different supports

In order to study the effect of support acidity, a new ZSM-5 based catalyst was prepared with SiO_2/Al_2O_3 ratio of 11 and the same procedure of 1.A. The global acid sites concentration is higher –as it was expected due to the lower Si/Al ratio-, but the strength of these sites is lower (Table 1). There are not important differences in the other characterization parameters. At 95% of C8 conversion, the yield of n-octane was 5.2 %, with 34.2 % of "C" and 23.5 % of "B". These results are congruent with the hypothesis that the acid sites stabilize the "C" intermediate, limiting the n-octane yield.

On the other hand, the small pores of these zeolites could introduce diffusional limitations. The larger molecular size of the hydrogenated furanic ring can also tune the formation and further transformation of the "C" intermediate. Zeolites L and K were chosen to study this effect. In both cases, ion exchange and nitrate precursor were used to prepare the supported catalysts. Considering the negative effect of acidity, Si/Al ratio was chosen in order to minimize the acidity of the zeolites. Organic supports were also considered testing the activity of Pt on active carbons (AC) and high surface area graphites (HSAG) as models of microporous and mesoporous materials, respectively. It was reported that active carbons exhibited some activity in hydrogenation reactions,[30] so their use as supports in hydrodeoxygenation could enhance the n-alkane yield. The problems derived of the microporous nature of the activated carbon (making difficult the accessibility of the reactants to the active phase) can be overcome using high-surface area graphites (HSAG). These materials are prepared by the

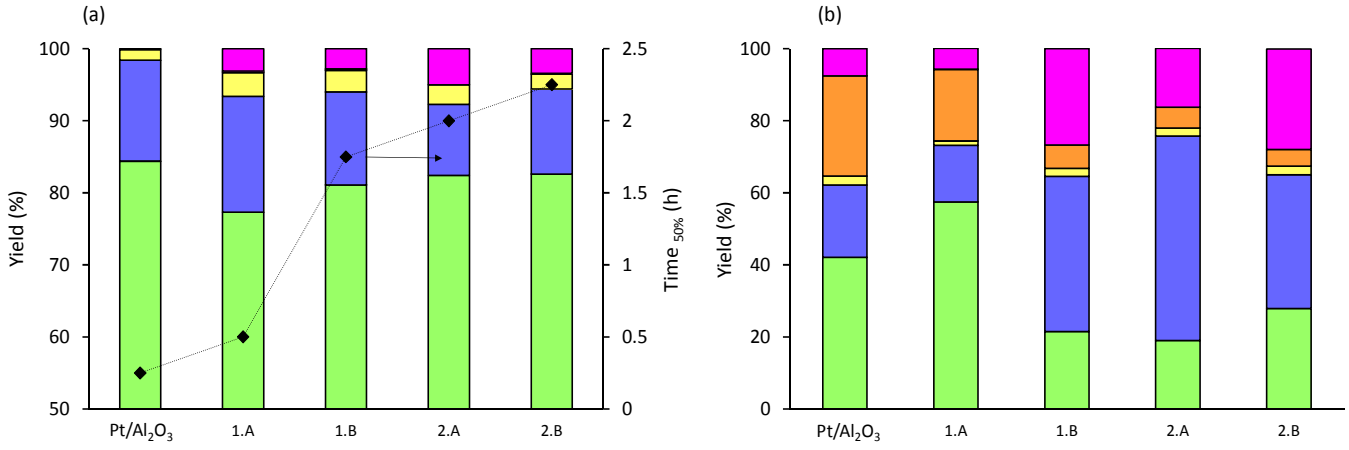

Figure 2: Comparison of yields obtained with the different Pt/ZSM-5 zeolites and Pt/Al_2O_3 at (a) 50 % of C8-condensated conversion and (b) after 24 hours of reaction. Colors: (●) "B"; (●) "C"; (●) "D"; (●) "E"; (●) "Carbon unbalance". Results related to the Pt/Al_2O_3 are adapted from *ref.13*.

mechanical modification of synthetic graphites, leading to disordered layers with oxygenated functional groups at the edges. These functional groups act as anchoring points that can activate the catalytic phase.[31]

In spite of the best results obtained with catalysts prepared by ion exchange, Pt/AC catalysts were prepared by both methods (ion exchange and incipient wetness), considering the low concentration of ions on its surface that can limit the Pt loading obtained by this method. MgZr mixed oxide and MgZr/HSAG500 were also chosen considering the good results obtained in the aldol condensation of furfural and acetone (reaction that produces the C8-condensated adduct).[5,6] Good results of these materials in the C8-condensated adduct HDO could be a starting point that allow considering both reaction as one step process.[32] The catalytic activity of all the supports (before impregnating with the Pt) has been tested, obtaining negligible formation of reaction products.

The main physicochemical properties of the resulting catalysts are summarized in the Table 1. Considering the heterogeneity of these supports, there are important differences in terms of surface area and pore volume. Regarding to the acidity, L and Y zeolites only show weak sites, whereas MgZr and carbon supported materials have weak and medium sites, with a density much lower than in ZSM-5 zeolites. Concerning the metal dispersion, similar results were obtained in all cases, with metal crystallites smaller than 10 nm, as it can be observed in Fig. S4-S5.

Figure 3 shows, for comparison, the yields obtained at 50 % of C8-condensated conversion and after 24 hours of reaction with these inorganic and organic supports. Results at 95 % of conversion are plotted in Fig. S6. The negative effect of the acidity, as well as the positive effect of HSAG as support (increasing the metal dispersion), were corroborated by the negligible yield of "C" obtained with Pt/HSAG and Pt/MgZr-HSAG, lower than 2.5 %. With these materials, most of the C8-condensated converted follows the direct reaction pathway A→B→D→E, preventing the B↔C equilibrium. Concerning the active carbons, it must be highlighted that the catalyst prepared by ion exchange is the most active, but this catalyst also favours some side-reactions or permanent adsorption.

After 24 hours of reaction, yields higher than 15 % of n-octane were obtained with alumina and carbonaceous materials (28 % with Pt/Al_2O_3, 16.9 % with Pt/HSAG, 21.4 % with Pt/MgZr/HSAG, 30.1 % with Pt/AC (WI) and 17.3 % with Pt/AC (IE)). Highest yield was obtained with active carbon, material showing the highest metal dispersion and almost negligible acidity. Final carbon balances obtained with Pt/L and Pt/Y decreased to 78.7 and 85 %, respectively, indicating the existence of permanent adsorption phenomenon or side reactions. This influence was much more important in the case of the activated carbons, with values of 63 % and 59 % with Pt/AC (WI) and Pt/AC (IE), respectively. On the other hand, these processes are less relevant in the case of Pt/MgZr, with a final carbon balance of 89.4 %, or the HSAG supported, with values of 93.8 % (Pt/HSAG) and 87 % (Pt/MgZr/HSAG500). Positive electronic interactions and affinities among the intermediates and the surface of mesoporous organic carbons can justify the good results obtained with these materials and the absence of a permanent adsorption that could limit the catalytic activity.[33]

Reaction kinetics

Results obtained are better explained applying a kinetic analysis. A reaction mechanism for the hydrodeoxygenation catalysed by different metals supported on alumina was proposed in our previous work.[13] This mechanism considers a set series-paraller steps with a first-order dependence respect to the condensation adducts and a negligible influence of the H_2 because of its large excess (with a decrease lower than 0.2 MPa after 24 h reaction time). Likewise, from results obtained with Pt catalysts,[13] the original kinetic

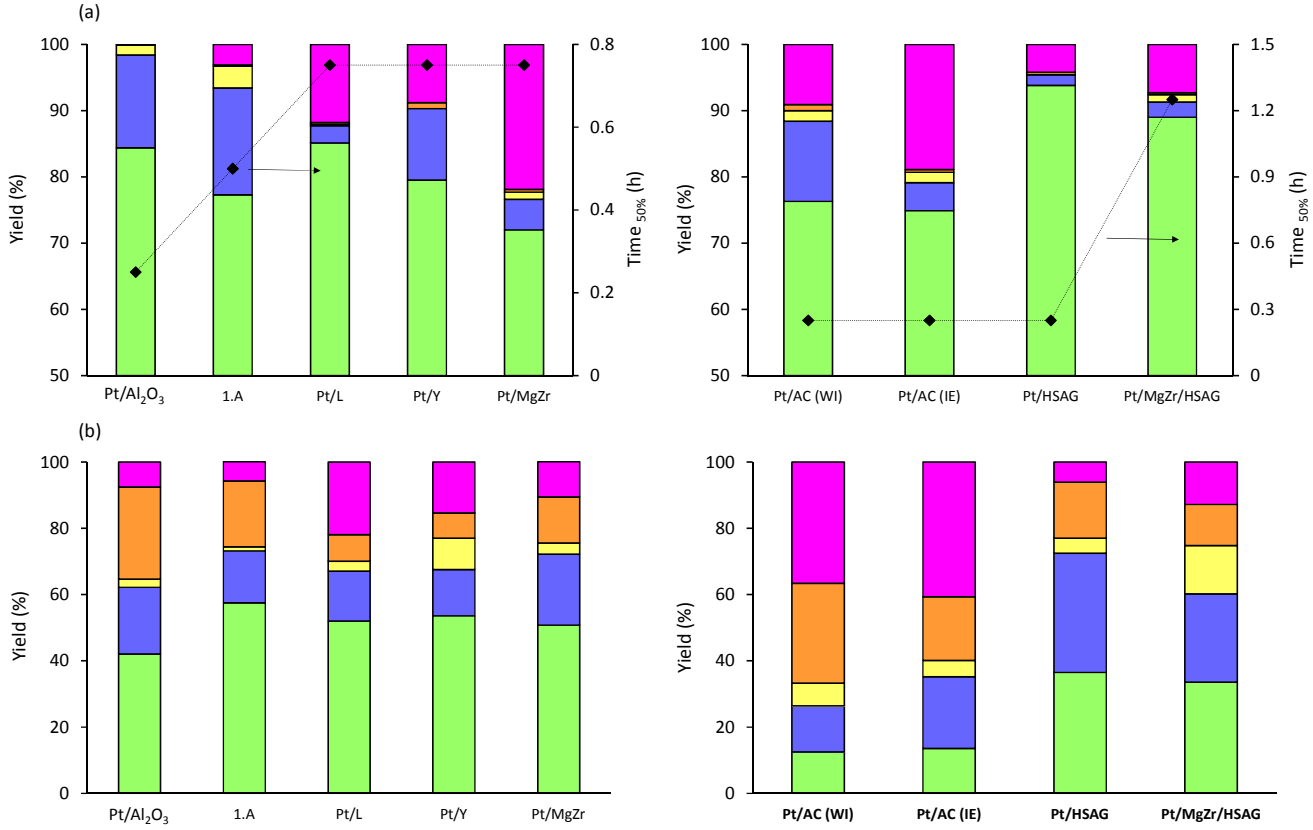

Figure 3: Comparison of yields obtained with the different inorganic and organic materials at (a) 50 % of f C8-condensated conversion and (b) after 24 hours of reaction. Colors: (●) "B"; (●) "C"; (●) "D"; (●) "E"; (●) "Others". Results related to the Pt/Al_2O_3 are adapted from *ref.13*.

mechanism was adapted and the general reaction network is summarized in Scheme 1. The reversibility/irreversibility of the different reaction steps have been determine in the basis of the temporal evolution of reaction products, since most of the reaction intermediates are not commercially available.

Side reactions were discarded considering the results obtained in the chemical analysis of the reaction mixture by GC-MS. It must be remarkable that no reaction products resulting from C-C bond cleavage were found. The decarbonylation was reported as the main side reaction in hydrodeoxygenations of carbonylic derivatives catalysed by VIII noble metals.[34,35] However, in these studies, the carbonyl function is a terminal aldehyde, whereas in the case of the C8 adduct, the aliphatic carbonyl involves an acetone molecule, decreasing the electropositive character of the carbonyl carbon and therefore preventing the C-C bond scission.

As well as in our previous work,[13] the presence of mass transfer effects was discarded by ensuring the small catalytic particle size (from 50 to 80 μm) and with the high stirring (1000 rpm), so this reaction is considered to be kinetically controlled. This hypothesis was corroborated by theoretical considerations for the estimation of mass-transfer effects in slurry reactors: the liquid-solid mass-transfer and the Thiele modulus-based efficiency factor for internal diffusion.[36] Results obtained confirm that the external mass transfer is largely faster than intrinsic reaction kinetics and the efficiency factor is close to one, so internal diffusion control was also discarded.

Contrary to alumina, the lower carbon balances obtained with some of the catalysts suggest the presence of permanent adsorption of at least one condensation adduct on the catalytic surface. The most representative temporal evolution of carbon balance are shown in Figure 4. The fast decrease of these profiles before the first hour of reaction indicates that the reactant (labelled as "A") is the main molecule adsorbed on the surface. This hypothesis is explained considering that the adsorption is favoured by C=C double bonds.[36] Consequently, an adsorption factor was added in the kinetic model (k_D), being the other kinetic constants the sketched in Scheme 1. The temporal evolution of the different compounds with reaction time was modelled using the SCIENTIST® software, applying the Burlich-Stoer approximation, and considering the following set of differential equations:

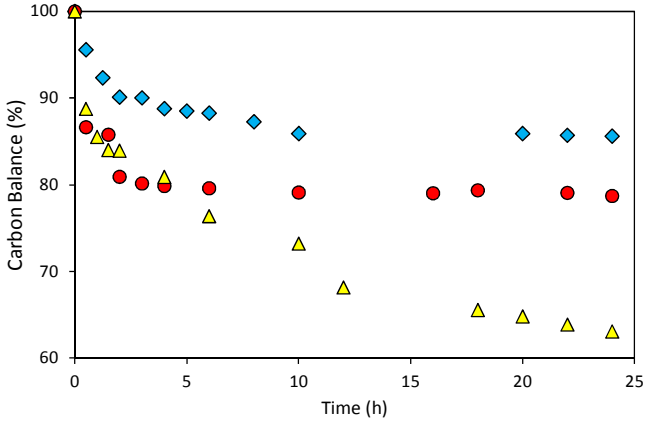

Figure 4: Temporal evolution of the carbon balance, considering the formation of the identified reaction products, for different catalysts: Pt/ZSM5-1:B (♦), Pt/L (●) and Pt/AC-WI (▲)

$$\frac{dA}{dt} = -k_1 \cdot A - k_D \cdot A \qquad \text{Eq: 1}$$

$$\frac{dB}{dt} = k_1 \cdot A - k_2 \cdot B - k_3 \cdot B + k_{-3} \cdot C \qquad \text{Eq: 2}$$

$$\frac{dC}{dt} = k_3 \cdot B - k_{-3} \cdot C \qquad \text{Eq: 3}$$

$$\frac{dD}{dt} = k_2 \cdot B - k_4 \cdot D \qquad \text{Eq: 4}$$

$$\frac{dE}{dt} = k_4 \cdot D \qquad \text{Eq: 5}$$

Values of the kinetic constants obtained with each catalyst are reported in Table 2. Considering that the adsorption is a surface process, the values of k_D were surface area normalized according to Eq. 6:

$$k'_D = \frac{k_D(s^{-1}) \cdot V(m^3)}{M_{cat}(g) \cdot S_{BET}(m^2/g)} \qquad \text{Eq: 6}$$

Where "k_D'" is the first-order adsorption constant expressed as meter per second; "k_D" is the first-order adsorption constant expressed in seconds, "V" is the reaction volume; "M_{cat}" is the mass of catalyst used in each reaction and "S_{BET}" is the specific surface area measured by physisorption.

On the other hand, the k_1, k_2, k_3, k_{-3} and k_4 values were normalized according to the following expression, considering the different metal loading and dispersion and, in order to provide a better comparison of the results:

$$k'\left(L \cdot s^{-1} \cdot atgr^{-1}{}_{met}\right) = \frac{k_D(s^{-1}) \cdot V(L)}{M_{cat}(g) \cdot (\%_{met}/100) \cdot (1/A_{met}) \cdot d} \qquad \text{Eq: 7}$$

Where "k'" is the first-order kinetic constant for a reaction rate expressed as mol reacted/formed per second and exposed atom of metal; "k" is the first-order kinetic constant for a reaction rate expressed in seconds, "M_{cat}" is the mass of catalyst used in each reaction; "A_{metal}" is the atomic mass of each metal; and "d" is the metal dispersion calculated by TEM.

As it can be observed in Table 2, good fits were obtained with all the materials, with a correlation coefficient higher than 0.94 in all the reactions. The values of kinetic constants suggest that there is more than one key parameter in this process and the final *n*-octane yield is the result of a balanced distribution of different catalyst properties.

Figure 5 shows the evolution of the different kinetic constants as a function of the crystallite particle size. These results suggest that the first step (hydrogenation of the aliphatic C=C) is clearly structure-sensitive, increasing the kinetic constant with the metal dispersion for all the supports. In general terms, it is accepted that the hydrogenation of C-C double bond is a structure insensitive reaction for small single molecules such as ethylene, but it tends to be structure sensitive as the size and the chemical complexity of the reactant increases, usually following a sympathetic behaviour, as the observed in our case.[38] It is not so easy to withdraw conclusions for the other kinetic constants, suggesting that the reaction is not only influenced by the properties of the metal active sites, but also by the chemistry of the support. Looking only at the effect of the metal dispersion, the hydrogenation of the aromatic ring seems to follow the opposite behaviour with respect to the first reaction, being increased both direct and reverse constant as the crystallite size increases. The relatively large molecular size as well as the polyfunctionalized structure of the reactant justifies the occupation of more than one metal site during the adsorption if the metal dispersion is not high enough and this blockage is more possible when the metal loading is higher. This fact was previously observed in other reactions.[39] In the case of the ring opening reaction, higher

Ca

Table 2: Kinetic constants k'_1-k'_4 ($L \cdot s^{-1} \cdot atm_{exp\_metal}$) and adsorption constant k'_D($m \cdot s^{-1}$) for the fitting experimental results at 493 K to the proposed kinetic model. *Results of Pt/Al_2O_3 are adapted from *ref. 13*.

	k'_1	k'_2	k'_3	k'_4	k'_{-3}	k'_D	r^2
Pt/Al_2O_3*	21.02	2.07	12.81	7.65	9.94	-	0.98
Pt/ZSM-5 (1.A)	9.36	0.18	4.14	0.95	5.44	$4.6 \cdot 10^{-12}$	0.96
Pt/ZSM-5 (1.B)	9.49	0.19	5.33	0.67	9.26	$1.7 \cdot 10^{-12}$	0.994
Pt/ZSM-5 (2.A)	7.26	0.18	6.26	0.23	12.59	$2.6 \cdot 10^{-12}$	0.993
Pt/ZSM-5 (2.B)	6.51	0.31	4.61	1.55	9.36	$2.8 \cdot 10^{-12}$	0.97
Pt/ZSM-5 (11)	7.82	0.29	3.43	1.63	7.20	$8.1 \cdot 10^{-13}$	0.996
Pt/L	7.91	0.15	7.76	0.52	6.34	$4.6 \cdot 10^{-12}$	0.996
Pt/Y	6.51	0.11	6.43	7.59	5.74	$3.9 \cdot 10^{-12}$	0.99
Pt/MgZr	8.20	0.09	4.48	4.46	3.90	$9.5 \cdot 10^{-12}$	0.98
Pt/HSAG500	8.91	0.37	3.22	5.58	6.57	$2.7 \cdot 10^{-12}$	0.98
Pt/AC (IE)	12.23	2.14	3.52	1.25	1.38	$7.9 \cdot 10^{-12}$	0.991
Pt/AC (WI)	15.21	1.14	0.57	1.18	1.26	$2.2 \cdot 10^{-11}$	0.94
Pt/MgZr/HSAG500	8.57	0.48	1.95	1.05	2.79	$2.2 \cdot 10^{-12}$	0.993

dispersion also seems to enhance the catalytic activity, although the trend is not as clear as in the case of the first hydrogenation. This fact suggests that the reaction mechanism is more complex, involving other catalyst functionalities.

Concerning the final hydrodeoxygenation (k_4), the observed trends are not so clear, suggesting that this step is not structure sensitive, and/or the reaction rate is controlled by other catalytic properties.

As to the influence of the catalyst morphology, the evolution of the kinetic constants with this parameter does not show any systematic trend, as it can be observed in Figure S7. Even more, higher kinetic constants were obtained (for similar dispersions) with those catalysts with the highest surface area and pore volume, suggesting again that this reaction is not limited by internal mass transfer effects, in spite of the relative large molecular size of the involved reactants.

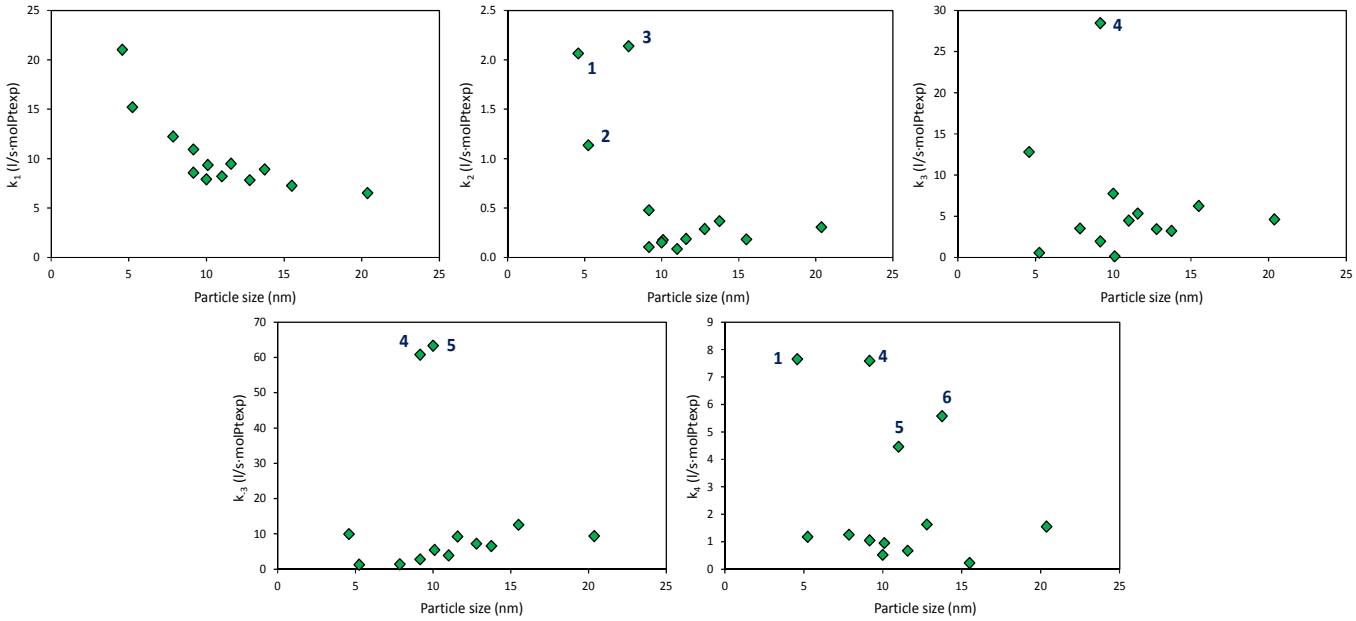

Figure 5: Correlation between the values of the kinetic constants and the Pt particle size of each catalyst. Codes: (1) Pt/Al_2O_3; (2) Pt/AC (WI); (3) Pt/AC (IE); (4) Pt/Y; (5) Pt/MgZr; (6) Pt/HSAG.

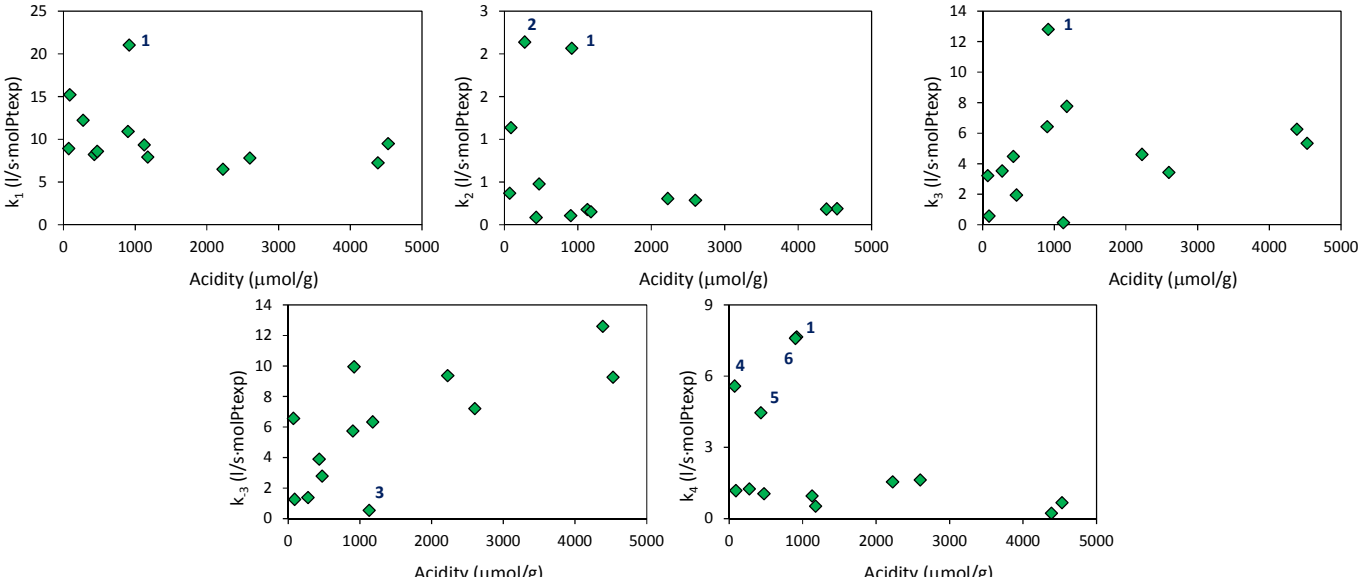

Figure 6: Correlation between the values of the kinetic constants and the acidity of each catalyst. Codes: (1) Pt/Al_2O_3; (2) Pt/AC (IE); (3) Pt/ZSM-5 (1.A); (4) Pt/HSAG; (5) Pt/MgZr; (6) Pt/Y.

According to the Figure 6, there is not a clear correspondence among the kinetic constants and the catalytic acidity. In good agreement with previous studies of hydrodeoxygenation reactions, the acidity does not play a key role in the hydrogenation.[40] The metal dispersion is so determining in the hydrogenation of the aliphatic insaturations that the influence of this parameter is not clear. On the other hand, it can be clearly observed that high concentration of acid sites (mainly strong sites) plays a negative effect in the furan cycle breaking-up (values of k_2) and stabilizes the furan. This fact is in good agreement with results previously observed in hydrogenations of cyclic compounds.[29] Concerning to the equilibrium between hydrogenation-dehydration of the furan cycle, both steps seems to be enhanced under acidic conditions, being this behaviour more clear in the case of the kinetic constant of the reverse reaction. However, the relevance of these values in the reaction rate is conditioned by the concentration of the reactive of each step, much higher in the case of direct path than in the indirect one. Taking this into account, these values are not strong enough for leading to a significant decomposition of the intermediate "C". Considering the whole process, it can be concluded that the activity is favoured by acid sites concentrations lower than 1000 µmol/g.

Catalytic stability

The catalytic stability was studied by carrying out six subsequent batch experiments at 493 K during 24 hours without any regeneration process (the catalyst was filtered after each batch, washed with distilled water and directly reused). The three most active catalysts were chosen to this study: Pt/Al_2O_3 (commercial sample), Pt/AC (WI) and Pt/HSAG500. In order to compare the reusability of these catalysts, Figure 7 shows the evolution of the yields obtained with each material in the first, third and sixth reaction cycles. Results are compared at the time at which 50 % of conversion were obtained and after 24 hours of reaction. Regarding to the carbon balance closure after the end of each cycle, in the case of the Pt/AC (WI) it keeps almost constant (from 63 % in the first

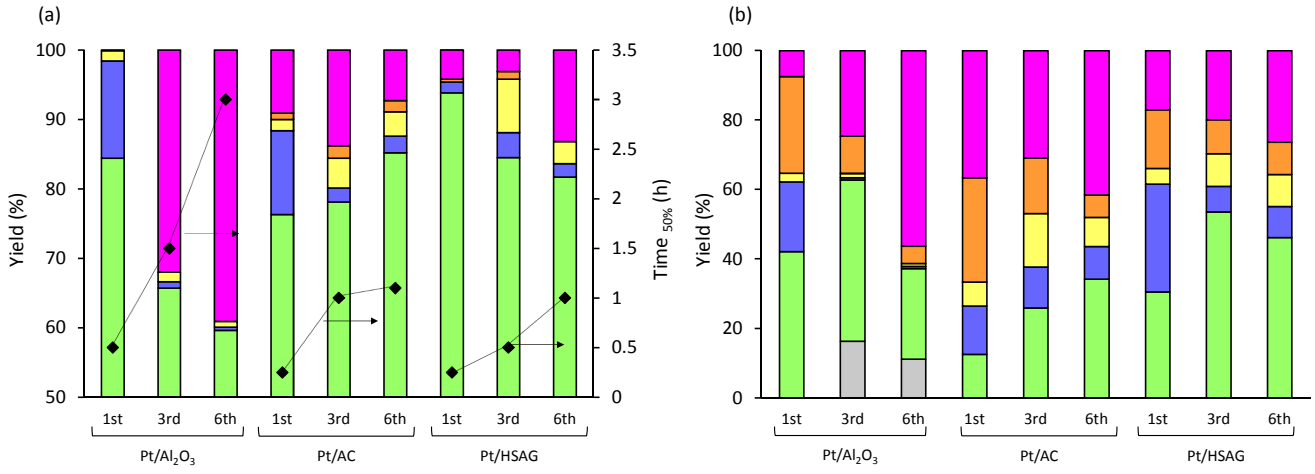

Figure 7: Comparison of the yields obtained after the first, third and sixth cycles of Pt/Al_2O_3, Pt/AC and Pt/HSAG catalysts at (a) 50 % of C8-condensated conversion and (b) after 24 hours of reaction. Colors: (●) "A"; (●) "B"; (●) "C"; (●) "D"; (●) "E"; (●) "Others".

cycle to 60.3 % in the last one) whereas there is an important decrease in the cases of the Pt/Al_2O_3 (from 89.3 to 74.5 %) and the Pt/HSAG500 (from 93.8 to 79.5 %).

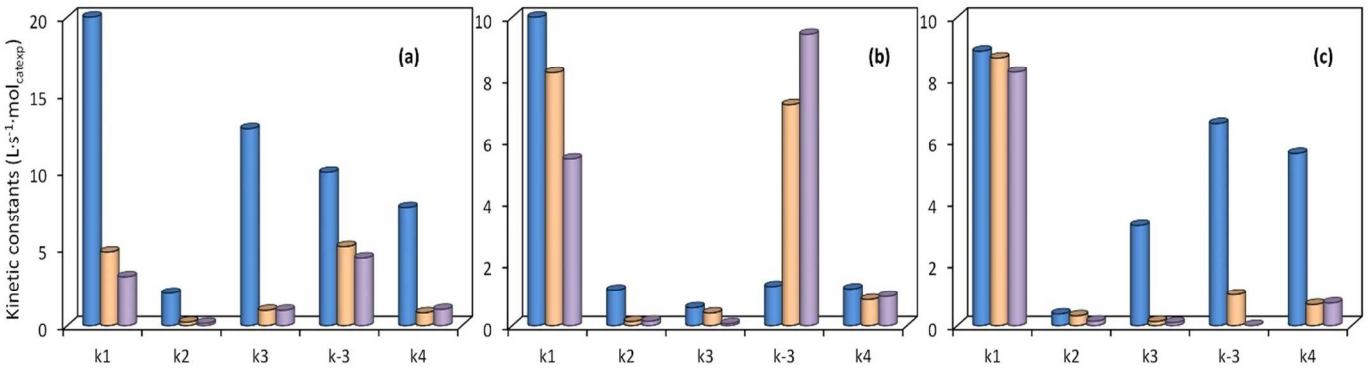

Figure 8: Evolution of the kinetic constants obtained in the reusability study: (a) Pt/Al_2O_3; (b) Pt/AC; (c) Pt/HSAG at 493 K. Results are reported for the first, third, and sixth cycle (from left to right)

Temporal profiles were successfully modelled considering the reaction mechanism proposed. Kinetic constants obtained are compared in Figure 8**,** obtaining correlations among fitted and experimental data with regression coefficient higher than 0.98 in all the cases.

In order determine the physicochemical causes of the deactivation, the spent catalysts (after the sixth cycle) were recovered and characterised by different techniques and main results are summarized in Table 3. Possible changes in the metal dispersion were analysed by transmission electron microscopy (TEM). TEM micrographs can be observed in Figure S8. In the three cases, small Pt particles can be observed, with negligible differences in the sizes between the fresh and the spent samples. These results suggest that metal particle sintering is not the cause of the deactivation of the catalysts.

In order to determine the presence of strongly adsorbed organics or coke deposits, the catalysts were characterized by TPO and nitrogen physisorption. In addition, used catalysts were leached in boiling hexane solution for 2 hours in a reflux system. The liquid phase was analysed by GC-MS, identifying in all the cases the C8 condensation adduct as the only organic compound. TPO experiments reveal the presence of organic compounds in the catalyst surface (Figure 9). That is more evident in the case of the Pt/Al_2O_3 catalyst, since the fresh catalyst does not present any combustion peak (as it is an inorganic catalyst) whereas the spent catalyst presents a significant CO_2 release peak (corresponding to a 2.3 % of C in the catalyst). The combustion temperature was higher than 750 K, indicating that these signals correspond to the combustion of compounds heavier than the C8-condensated, which has a combustion temperature of 700 K.[5]

In the same way, the morphology of this catalyst changes slightly upon reaction (Table 3), leading to lower surface area, a marked decrease in pore volume and diameter. This is in good agreement with the expected behaviour of alumina-supported catalyst, as showed in other hydrogenation reactions.[41] As it is a slightly acid and mesoporous support, it can promote the formation of carbonaceous deposits, but these deposit cannot block entire pores. For the other supports, it should be taken into account that supports also undergo combustion. In spite of this, in the case of the activated carbon support, the CO_2 release corresponding to the spent catalyst is largely higher than the corresponding to the fresh catalyst, suggesting that the catalyst contains a large amount of adsorbed organic matter. In good agreement with this fact, the morphology of the catalyst markedly changes after reaction, with a decrease of more than 40 % of the surface area. It should be noted that, in the case of a microporous materials, the carbonaceous material can block micropores, decreasing the surface more sharply.[42] In the case of the HSAG-supported catalysts, the TPO profiles of the fresh and spent catalysts are rather similar, suggesting that the amount of carbon deposits is largely lower than in the case of the other two catalysts. In the case of surface area, the changes are quantitatively lower than in the case of the Pt/AC but more important than for the alumina-supported catalysts. In the leaching experiments the concentration of

Table 3: Morphological and physico-chemical parameters of the fresh and after six reaction cycles. *Data adapted from *ref.13*

	N_2 physisorption			TEM		Lixiviation (mmol A/g_{cat})	TPO results ($mmolCO_2/g$)
	S_{BET} (m^2/g)	d_p (nm)	v_p (cm^3/g)	dc (nm)	D (%)		
Pt/Al_2O_3 fresh*	116	17.0	0.49	4.6	23.9	-	0.05
Pt/Al_2O_3 used	105	6.9	0.26	5.2	21.0	0.088	15.4
Pt/AC (WI) fresh	1716	1.9	0.59	5.2	21.3	-	0.5
Pt/AC (WI) used	1049	1.6	0.33	7.1	15.5	0.58	339.6
Pt/HSAG500 fresh	498	7.6	0.67	13.8	8.6	-	0.2
Pt/HSAG500 used	385	6.3	0.21	14.2	7.7	0.57	92.8

organic species is similar for both organic supports and one order of magnitude lower for the alumina-supported catalyst.

Catalyst performance and characterization results can be discussed in terms of the kinetic constants shown in Fig. 8. Looking at the first reaction step (k_1), the hydrogenation of the aliphatic C-C double bond, the Pt/Al_2O_3 shows the sharpest decrease in the reaction rate during the reaction, being this decrease almost negligible for the case of the HSAG-supported catalyst, whereas for the Pt/Al_2O_3 it follows an intermediate behaviour (as shown in Fig. 8). These results suggest that the formation of carbonaceous deposits or the irreversible adsorption of reaction intermediates on the active phase is more important on the alumina-supported catalysts. Therefore, although carbonaceous supports bear higher amounts of these undesired organics, they are unspecifically placed, because of the high affinity for hydrophobic organic surfaces.

Concerning the ring-opening reaction (k_2), both Pt/Al_2O_3 and Pt/AC present very similar behaviour, with strong deactivation, whereas the decrease is more slight for the HSAG-supported catalyst. In the case of the reversible reaction of ring hydrogenation, in all the catalyst the formation of this intermediate "C" is hindered as the catalyst is deactivated (k_{-3} decreases more slightly than k_3 or even increases as the catalyst is deactivated). As a result, the yield for "C" intermediate formation largely decreases for Pt/Al_2O_3 and Pt/AC and remains almost constant for the Pt/HSAG catalyst. The behaviour of the reaction steps 2 and 3, is good agreement with the lower specificity for this reaction, leading to a key role of support properties in the reaction.

The behaviour of the last reaction step (the hydrodeoxygenation of the diol intermediate "D"), is completely different, since both AC- and alumina-supported catalysts present very similar behaviour, whereas the decrease of the value of this kinetic constant is more marked for the HSAG-based catalysts. This effect is explained considering that this final step requires both metallic sites (for activating hydrogen) and acid sites, as the hydroxyl groups of the alumina or acid organic functional groups of the activated carbons. HSAG presents lower concentration of these sites than AC, and therefore it is more sensitive to the blocking of these functional groups. In good agreement, the yield of n-octane presents the most marked decrease for the HSAG catalyst (Fig. 8), in spite of the better behaviour of this catalyst for the previous steps.

Conclusions

Reported data suggest that metal dispersion plays a key role in the HDO, whereas support chemistry plays a secondary role. The acidity of the support has not only any positive effect on the yield to hydrocarbon product, but also promotes the formation of unreactive intermediates and the irreversible adsorption of reactants and products. Regarding to organic supports, the positive effect in avoiding lateral reactions is partially overlapped with the highest trend to bear irreversible adsorption, especially for the activated carbon, because of its microporous character. High surface area graphite presents an intermediate behaviour, which becomes it in a promising support.

Kinetic analysis of the catalysts performance with fresh and re-used catalyst suggests three factors that influence the catalytic steps: catalyst dispersion, distribution of acid sites and adsorptive behaviour of the catalysts.

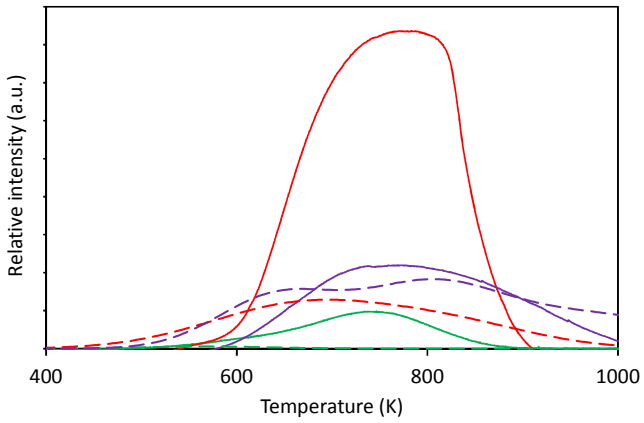

Figure 9: CO_2 releasing profiles for the TPO of the fresh and used catalysts used for the stability studies. Colors: (■) Pt/Al_2O_3; (■) Pt/AC; (■) Pt/HSAG.

Acknowledgements

This work was supported by the Spanish Government (contract CTQ2011-29272-C04-02). HSAG supports were a generous gift of Timcal.

Notes and references

[a] Department of Chemical and Environmental Engineering. Faculty of Chemistry, University of Oviedo, Julián Clavería s/n, 33006 Oviedo, Spain. Tel: (+) 34 985103437. Fax: (+) 34 985103434. Email: sordonez@uniovi.es.

Electronic Supplementary Information (ESI) available: TEM micrographs of the catalysts, additional data comparing yields to the different products at 95 % conversion, correlation between kinetic constants and morphological parameters. See DOI: 10.1039/b000000x/

1. R. Rinaldi, F. Schüth, *ChemSusChem*, 2009, **2**, 1096.
2. G.W. Huber, J.N. Chheda, C.J. Barrett, J.A. Dumesic, *Science*, 2005, **308**, 1446.
3. H. Olcay, A.V. Subrahmayan, R. Xing, J. Lajoie, J.A. Dumesic, G.W. Huber, *Energy Environ. Sci.*, 2013, **6**, 205.
4. C. García-Sancho, I. Agirrezabal-Tellería, M.B. Güemez, P. Maireles-Torres, *Appl. Catal. B*, 2014, **152-153**, 1.
5. L. Faba, E. Díaz, S. Ordóñez, *Appl. Catal. B*, 2012, **113-114**, 201.
6. L. Faba, E. Díaz, S. Ordóñez, *ChemSusChem*, 2013, **6**, 463.
7. M.J. Climent, A. Corma, S. Iborra, *Green Chem.* 2014, **16**, 516.
8. I. Sadaba, M. Ojeda, R. Mariscal, J.L.G. Fierro, M.L. Granados. *Appl. Catal. B*, 2011, **101**, 638.
9. S.A. Qader, G.R. Hill, *Ind. Eng. Chem. Proc. Des. Dev.*, 1963, **8(4)**, 451.
10. J.N. Chheda, D.A. Dumesic, *Catal. Today*, 2007, **123**, 59.
11. S. Sittisa, T. Pham, T. Prasomsri, T. Sooknoi, R.G. Mallinson, D.E. Resasco, *J. Catal.*, 2011, **280**, 17.
12. J. He, C. Zhao, J.A. Lercher, *J. Catal.*, 2014, **309**, 362.
13. L. Faba, E. Díaz, S. Ordóñez, *Appl. Catal. B*, 2014, **160-161**, 436.
14. Y. Zhang, D. Kang, C. Saquing, M. Aindow, C. Erkey, *Ind. Eng. Chem. Res.*, 2005, **4,** 4161.
15. M. Abid, R. Touroude, *Catal. Lett.*, 2000, **69**, 139.
16. F. Ammari, J. Lamotte, R. Touroude, *J. Catal.*, 2004, **221**, 32.
17. P. Mäki-Arvela, J. Hájek, T. Salmi, D. Yu. Murzin, *Appl. Catal. A*, 2005, **292**, 1.
18. R.V. Malyala, C.V. Rode, M. Arai, S.G. Hegde, R.V. Chaudhari, *Appl. Catal. A*, 2000, **193**, 71.
19. P. Mäki-Arvela, L-P. Tiainen, M. Lindblad, K. Demirkan, N. Kumar, R. Sjöholm, T. Ollonqvist, J. Väyrynen, T. Salmi, D. Yu. Murzin, *Appl. Catal. A*, 2003, **241**, 271.
20. B. Bachiller-Baeza, A. Guerrero-Ruiz, P. Wang, I. Rodríguez-Ramos, *J. Catal.*, 2001, **204**, 450.
21. S. Ordóñez, E. Díaz, R.F. Bueres, E. Asedegbega-Nieto, H. Sastre, *J. Catal.*, 2010, **272**, 158.

22. R.D. Clayton, M.P. Harold, V. Balakotaiah, C.Z. Wan, *Appl. Catal. B*, 2009, **90**, 662.
23. M. Göhlich, S. Böttcher, K. Räuchle, W. Reschetlowski, *Catal. Commun.*, 2011, **12**, 757.
24. P. Cañizares, A. de Lucas, F. Dorado, A. Durán, I. Asencio, *Appl. Catal. A*, 1998, **169**, 137.
25. A.R. Vaccaro, G. Mul, J. Pérez-Ramírez, J.A. Moulijn. *Appl. Catal. B,* 2003, **46**, 687.
26. K. Hayek, H. Goller, S. Penner, G. Rupprechter, C. Zimmermann. *Catal Lett*. 2004, **92**, 1.
27. D-K. Lee, S-K. Ihn, *J. Catal.* 1987, **106**, 386.
28. B. Pawelec, R. Mariscal, R.M. Navarro, S. van Bokhorst, S. Rojas. J.L.G. Fierro. *Appl. Catal. A*, 2002, **225**, 223.
29. F.C.A. Figuereido, E. Jordao, R. Landers, W.A. Carvalho, *Appl. Catal. A*, 2009, **371**, 131.
30. Z-G. Zhang, K. Okada, M. Yamamoto, T. Yashida, *Catal. Today*, 1998, **45**, 361.
31. E. Díaz, S. Ordóñez, R.F. Bueres, E. Asedegbega-Nieto, H. Sastre, *Appl. Catal. B*, 2010, **99**, 181.
32. L. Faba, E. Díaz, S. Ordóñez, *ChemSusChem*, 2014, **7**, 2816.
33. V. Ponec, *Appl. Catal. A*, 1997, **149**, 27.
34. T.T. Pham, L.L. Lobban, D.E. Resasco, R.G. Mallinson, *J. Catal.*, 2009, **266**, 9.
35. J. Lee, Y. Xu, G.W. Huber, *Appl. Catal. B*, 2013, **140-141**, 98.
36. H.S. Fogler, M.N. Gürmen, *Elements of Chemical Reaction Engineering*, ed. Pearson, 4Ed, 2008, ch. 11.
37. J.I. Di Cosimo, A. Acosta, C.R. Apesteguia, *J. Mol. Catal. A*, 2005, **234**, 111.
38. J.A. Bennett, R. P. Fishwick, R. Spence, J. Wood, J.M. Winterbottom, S.D. Jackson, E.H. Stitt, *Appl. Catal. A*, 2009, **364**, 57.
39. A. Jong, A. Jess, T. Schubert, W. Schütz, *Appl. Catal. A*, 2009, **362**, 95.
40. J.A. Dumesic, Y. Roman-Leshkov, *US 2009/0124839*.
41. S. Ordóñez, H. Sastre, F.V. Díez, *Thermochim. Acta*, 2001, **379**, 25.
42. S. Ordóñez, F.V. Díez, H. Sastre, *Appl. Catal. B*, 2001, **31**, 113.

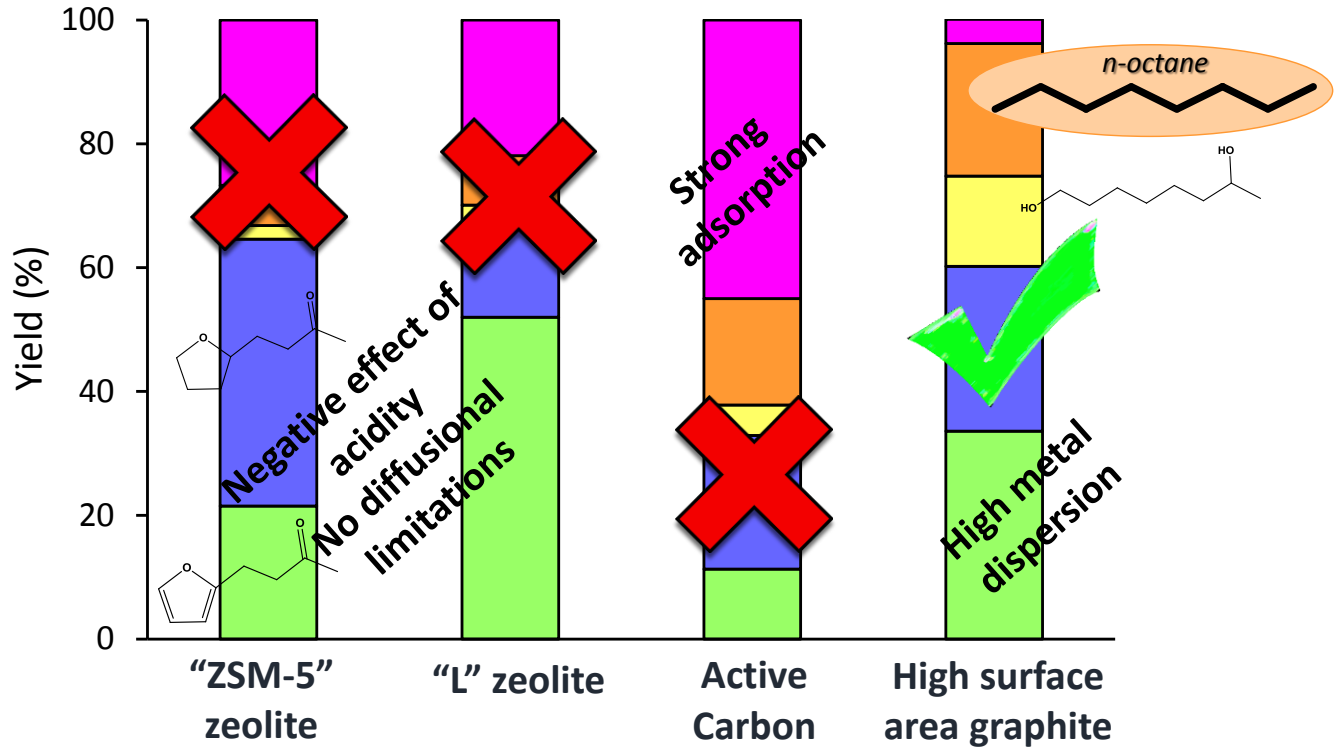

The roles of metal dispersion and support properties of Pt catalysts on their performance for HDO of condensation adducts has been determined.